Imaging a dam-rock interface with inversion of a full elastic-acoustic model

Mohamed Aziz Boukraa, Marcella Bonazzoli, Houssem Haddar, Lorenzo Audibert, Denis Vautrin

11th International Conference on Inverse Problems in Engineering
June 23-28, 2024, Búzios, Rio de Janeiro, Brazil

ICIPE–2024–0116
Imaging a dam-rock interface with inversion of a full elastic-acoustic model

Mohamed Aziz Boukraa
Marcella Bonazzoli
Houssem Haddar
UMA, INRIA, ENSTA Paris, Institut Polytechnique de Paris, 91120 Palaiseau, France
mohamed.boukraa@inria.fr, marcella.bonazzoli@inria.fr, houssem.haddar@inria.fr

Lorenzo Audibert
Denis Vautrin
EDF R&D, département PRISME, bâtiment U, 6 quai Watier, BP 49, 78401 Chatou Cedex, France
lorenzo.audibert@edf.fr, denis.vautrin@edf.fr

Abstract. *We are interested in imaging the interface between the concrete structure of hydroelectric dams and the rock foundation using non-destructive seismic waves. We present a geophysical technique for processing seismic measurements to obtain an image of the interface with metric resolution. The proposed technique is based on "Full Waveform Inversion" with a shape optimization approach. Numerical results using synthetic measurements demonstrate the method ability to accurately recover the interface with a limited number of measurement points and in the presence of noise.*

Keywords: *Geophysics, subsurface imaging, Full Waveform Inversion, seismic measurement, non-destructive evaluation.*

1. INTRODUCTION

In the context of studying the stability of hydroelectric dams, the ability to retrieve the shape of the contact between the dam and the rock foundation is of a great importance. It represents a key factor for assessing the understanding of the mechanical behavior of dams in relation with the pressure exerted by the retained water, and thus for identifying additional margins regarding their stability.

To address this issue, subsurface imaging methods can be employed. Traditionally, geotechnical techniques, such as core drilling are performed. However, this can be invasive in some cases and only provide specific and limited information, making the extrapolation to the entire structure challenging.

The current approach under study involves exploring geophysical measurement techniques to obtain a non-destructive 2D image of the bottom of the excavation. This study concerns the case of gravity dams, since their shape can be considered approximately invariant along their longitudinal direction.

Geophysical measurement techniques can provide additional information to geotechnical measurements and are cost-effective. This would refine the knowledge of the interface geometry and limit the number of on-site drillings. We are particularly interested in seismic imaging techniques.

On-site experiments for acquiring seismic measurements involve exciting the dam structure on its surface or generating over-pressure in the water. Receivers are deployed on both faces to capture both direct and reflected waves. Immersed receivers are positioned on the upstream side to capture water pressure.

Based on synthetic signals and measurements taken at an actual site, two processing techniques, namely Seismic Reflection and Vertical Seismic Profile have been tested. However, this has not yielded satisfactory results. This highlights the complexity of the problem, attributed in part to the intricate geometry of the structure. Consequently, conventional processing methods are not suitable for this issue.

Therefore, to be able to image the concrete/rock interface with satisfactory spatial resolution, it is necessary to implement more advanced techniques capable of faithfully considering the structure geometry and the complexity of the resulting wave propagation modes.

In this work, we present an imaging method based on the "Full-Waveform Inversion" (FWI) technique as introduced by Lailly (1983) and Tarantola (1984). Our approach involves modeling seismic wave propagation in the solid structure (the dam and the underlying rock) and the water medium through an Elastic-Acoustic model solved using the Finite Element Method (FEM). Additionally, we develop an inversion method incorporating geometric shape optimization techniques. In this strategy, the gradient of the cost functional is computed using the method proposed by Cea (1986), while the formulation for shape derivatives can be referenced from the book of Allaire and Schoenauer (2006). Numerical results applied to simulated measurements demonstrate the method accuracy in retrieving the shape of the interface in two dimensions,

showcasing its robust performance even with a limited number of measurement points and in the presence of noise.

2. Statement of the model problem

We describe the responses to excitation as solutions to frequency-domain wave propagation problems, which are the linear elasticity problem in the solid medium, and the acoustics problem in the water medium (the reservoir), with suitable transmission boundary conditions at the interface between the two media. The 2D computational domain is a vertical section of the dam and the surrounding media (see Fig. 1), since the shape of gravity dams can be considered approximately invariant along their longitudinal direction. The current model does not account for dissipation, and both the dam and rock materials are assumed to be isotropic and homogeneous.

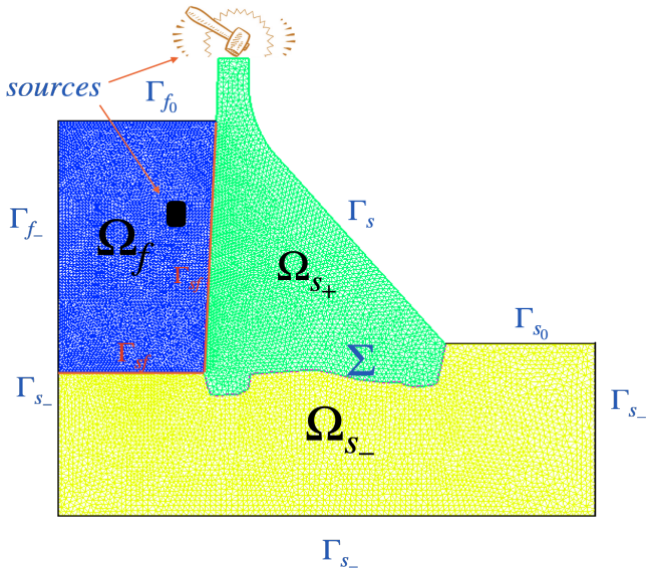

Figure 1: 2D schematic diagram for the considered excitations of the dam structure, the water and the rock foundation.

In the presence of water in the dam reservoir, two types of source are considered: $\vec{g_s}$ for an emerged source on the emerged wall Γ_s, or g_f for an immersed source in the water medium Ω_f. In the on-site experiments these two types of source are not activated simultaneously, so either $\vec{g_s}$ or g_f is zero. We denote by Ω_{s_+} the dam medium, Ω_{s_-} the rock medium, and Σ the interface between the dam and the rock. The solid medium is represented by $\Omega_s = \Omega_{s_+} \cup \Omega_{s_-} \cup \Sigma$. The entire domain is denoted by $\Omega = \Omega_s \cup \Omega_f$. The wave propagation is described by the elasto-acoustic model, which couples the linear elasticity equation for the displacement vector $\vec{u}$ in Ω_s and the Helmholtz equation for the pressure p in Ω_f:

$$\begin{cases} \nabla \cdot \underline{\underline{\boldsymbol{\sigma}}}(\vec{u}) + \rho\omega^2\vec{u} = 0 & \text{in } \Omega_s \\ \Delta p + k^2 p = g_f & \text{in } \Omega_f \\ \rho_f \omega^2 \vec{u}\cdot\vec{n} = \nabla p \cdot \vec{n} & \text{on } \Gamma_{sf} \\ \underline{\underline{\boldsymbol{\sigma}}}(\vec{u})\vec{n} = -p\vec{n} & \text{on } \Gamma_{sf} \\ \underline{\underline{\boldsymbol{\sigma}}}(\vec{u})\vec{n} = \vec{g_s} & \text{on } \Gamma_s \\ \underline{\underline{\boldsymbol{\sigma}}}(\vec{u})\vec{n} = 0 & \text{on } \Gamma_{s_0} \\ \nabla p \cdot \vec{n} = 0 & \text{on } \Gamma_{f_0} \\ \vec{u}|_{\Omega_{s_-}} & \text{is outgoing} \\ p|_{\Omega_f} & \text{is outgoing} \end{cases} \tag{1}$$

In the elasto-acoustic system (1), $\underline{\underline{\boldsymbol{\sigma}}}(\vec{u})$ is the stress tensor (which is a 2×2 matrix) defined as follows:

$$\begin{aligned} \underline{\underline{\boldsymbol{\sigma}}}(\vec{u})|_{\Omega_{s_\pm}} &= E_{ijkl} u_{k,l}, \\ E_{ijkl} &= \mu_\pm(\delta_{ik}\delta_{jl} + \delta_{il}\delta_{jk}) + \lambda_\pm \delta_{ij}\delta_{kl} \quad \text{for } i,j,k,l \in \{1,2\}, \\ u_{k,l} &= \frac{\partial u_k}{\partial x_l}, \end{aligned} \tag{2}$$

where we make use of the Einstein summation convention, δ_{ij} is the Kronecker delta, $\mu_\pm$ and $\lambda_\pm$ are the Lamé constants of the dam concrete in Ω_{s_+} and of the rock foundation in Ω_{s_-}. In the full solid region Ω_s the physical parameters are denoted without indexes as $\mu = \mu_+ \mathbf{1}_{\Omega_{s_+}} + \mu_- \mathbf{1}_{\Omega_{s_-}}$ and $\lambda = \lambda_+ \mathbf{1}_{\Omega_{s_+}} + \lambda_- \mathbf{1}_{\Omega_{s_-}}$ (where $\mathbf{1}_A$ is the indicator function of a set A). In the linear elastic equation, $\overline{\nabla}\cdot$ denotes the divergence operator for tensors, which is defined as the vector:

$$\nabla \cdot \underline{\underline{\boldsymbol{\sigma}}} = \sum_{j=1}^{2} \frac{\partial \sigma_{ij}}{\partial x_j} e_i, \text{ for } i \in \{1, 2\},$$

where e_i is the elementary vector. In the acoustic equation, k represents the wave number in the water medium, and ρ_f is the water mass density.

Two transmission boundary conditions are set on the interface between the solid and water media Γ_{sf}. We also consider the following notation for the remaining boundary parts as described in Fig. 1:

$$\Gamma_s = \partial\Omega_{s_+} \setminus \{\Sigma, \Gamma_{sf}\}, \quad \Gamma_{s_0} \cup \Gamma_{s_-} = \partial\Omega_{s_-} \setminus \{\Sigma\}, \quad \Gamma_{f_0} \cup \Gamma_{f_-} \cup \Gamma_{sf} = \partial\Omega_f.$$

The outgoing condition is modeled using the PML (Perfectly Matched Layers) technique (see e.g. Michler *et al.* (2007)), which is used to truncate the unbounded physical domain and solve an approximate problem posed on a bounded computational domain. Moreover, Dirichlet boundary conditions are added on the PML borders ($\vec{u} = 0$ on Γ_{s_-} and $p = 0$ on Γ_{f_-}).

3. The inverse problem

To image the dam-rock interface we use a quantitative inversion algorithm: the Full Waveform Inversion (FWI) method, which was first introduced in the work of Lailly (1983) and Tarantola (1984). It has been influenced by the contributions of various geophysicists and researchers in the field of seismic inversion techniques.

This method relies on seismic or acoustic measurements, which, as a first validation step of our work, are constructed numerically, using model (1). The interface shape is iteratively updated to minimize the cost functional that computes the misfit between the (synthetic) measurements and those obtained by simulating the wave propagation models for a current tentative shape (on a mesh different from the one used to construct the synthetic measurements). This shape optimization process is performed by a gradient descent algorithm.

More precisely, given M source terms $g_1, \ldots, g_M$ (where this generic notation indicates any of the vector/scalar sources $\vec{g_s}, g_f$ of problems (1)), the inverse problem consists in determining the interface Σ_{ex} from (possibly noisy) measurements:

$$\vec{u^1}_{\text{mes}} \simeq \vec{u}_1(\Sigma_{\text{ex}})|_{\Gamma_{ms}}, \ldots, \vec{u^M}_{\text{mes}} \simeq \vec{u}_M(\Sigma_{\text{ex}})|_{\Gamma_{ms}},$$
$$p^1_{\text{mes}} \simeq p_1(\Sigma_{\text{ex}})|_{\Gamma_{mf}}, \ldots, p^M_{\text{mes}} \simeq p_M(\Sigma_{\text{ex}})|_{\Gamma_{mf}},$$

where $\Gamma_{ms} \subset \Gamma_s$ and $\Gamma_{mf} \subset \Gamma_{sf}$ are the measurements locations. The interface Σ_{ex} is approximated by solving a shape optimization problem for a given set of admissible shapes $\boldsymbol{\mathcal{U}}_{\text{admissible}}$:

$$\begin{cases} \text{Find } \Sigma_{\text{opt}} \in \boldsymbol{\mathcal{U}}_{\text{admissible}} \text{ such that} \\ \quad \Sigma_{\text{opt}} = \underset{\Sigma \in \boldsymbol{\mathcal{U}}_{\text{admissible}}}{\text{argmin}} \; J(\Sigma), \end{cases}$$

where we consider the following objective functional:

$$J(\Sigma) = \frac{1}{2} \sum_{i=0}^{M} \|\vec{u^i}(\Sigma)|_{\Gamma_{ms}} - \vec{u^i_{\text{mes}}}\|^2_{L^2(\Gamma_{ms})} + \frac{1}{2} \sum_{i=0}^{M} \|p^i(\Sigma)|_{\Gamma_{mf}} - p^i_{\text{mes}}\|^2_{L^2(\Gamma_{mf})} + \eta R(\Sigma). \tag{3}$$

The objective functional (3) includes misfit terms denoted by $J_d(\Sigma)$, contributing to identifying the optimal shape that best aligns the synthetic measurement with the real measurement:

$$J_d(\Sigma) = \frac{1}{2} \sum_{i=0}^{M} \|\vec{u^i}(\Sigma)|_{\Gamma_{ms}} - \vec{u^i_{\text{mes}}}\|^2_{L^2(\Gamma_{ms})} + \frac{1}{2} \sum_{i=0}^{M} \|p^i(\Sigma)|_{\Gamma_{mf}} - p^i_{\text{mes}}\|^2_{L^2(\Gamma_{mf})}, \tag{4}$$

and a perimeter regularization term $R(\Sigma) = |\Sigma|$, weighted by the regularization parameter $\eta \geq 0$. This regularization contributes in smoothing the reconstruction of the interface by mitigating uncertainties arising from potentially noisy and sparse data.

Shape optimization methods differ significantly from classical optimization techniques because they involve differentiating with respect to the shape to compute the gradient of the functional, whose explicit expression can be challenging

to obtain (see e.g. Allaire and Schoenauer (2006)). To derive the expression of the shape gradient, we employ the method introduced by Cea (1986), which utilizes a Lagrangian technique as a tool to obtain shape derivatives without the need for explicit computation. This method requires solving both a direct problem and an adjoint problem. For a given mesh Ω with interface Σ, we denote $(\vec{u}_\Omega, p_\Omega)$ the solution of the direct problem (1). Following Céa's method, the adjoint state $(\vec{v}_\Omega, q_\Omega)$ is obtained by solving the following adjoint problem:

$$\begin{cases} \nabla \cdot (\underline{\underline{\boldsymbol{\sigma}}}(\vec{v}_\Omega)) + \rho\omega^2 \vec{v}_\Omega = 0 & \text{in } \Omega_s \\ \Delta q_\Omega + k^2 q_\Omega = 0 & \text{in } \Omega_f \\ -\vec{v}_\Omega \cdot \vec{n} = \dfrac{\partial q_\Omega}{\partial n} - \overline{\left(p_\Omega|_{\Gamma_{mf}} - p_{\text{mes}}\right)} & \text{on } \Gamma_{mf} \\ \underline{\underline{\boldsymbol{\sigma}}}(\vec{v}_\Omega)\vec{n} = \rho_f \omega^2 q_\Omega \vec{n} & \text{on } \Gamma_{sf} \\ \underline{\underline{\boldsymbol{\sigma}}}(\vec{v}_\Omega)\vec{n} = -\overline{\left(\vec{u}_\Omega|_{\Gamma_{ms}} - \vec{u}_{\text{mes}}\right)} & \text{on } \Gamma_s \\ \underline{\underline{\boldsymbol{\sigma}}}(\vec{v}_\Omega)\vec{n} = 0 & \text{on } \Gamma_{s_0} \\ \nabla q_\Omega \cdot \vec{n} = 0 & \text{on } \Gamma_{f_0} \end{cases} \tag{5}$$

In our approach, we assume perfect knowledge of the geometry of the dam, as well as the physical parameters of each material. Our inversion method relies on considering the shape of the interface as the sole unknown. Therefore, when applying the shape derivative theorem (see e.g. Allaire and Schoenauer (2006)), we can choose a direction $\vec{h}$ supported only on the interface Σ. The shape derivative of the misfit functional is then restricted only to Σ and is given by the following integral:

$$J'_d(\Sigma)(\vec{h}) = \int_\Sigma \mathrm{Re}(j(\Sigma))\vec{h} \cdot \vec{n}\, ds,$$

where

$$\begin{aligned} j(\Sigma) = &\Big(\Theta_+(\vec{u}_{\Omega_{s_+}}) : \Theta_+(\vec{v}_{\Omega_{s_+}})\Big) - \Big(\Theta_-(\vec{u}_{\Omega_{s_-}}) : \Theta_-(\vec{v}_{\Omega_{s_-}})\Big) - \omega^2\Big(\rho_{s_+}(\vec{u}_{\Omega_{s_+}} \cdot \vec{v}_{\Omega_{s_+}}) \\ &- \rho_{s_-}(\vec{u}_{\Omega_{s_-}} \cdot \vec{v}_{\Omega_{s_-}})\Big), \\ \Theta_\pm(\vec{u}_{\Omega_{s_\pm}}) = &\lambda_{\Omega_{s_\pm}} \mathrm{div}(\vec{u}_{\Omega_{s_\pm}})\mathrm{Id} + 2\mu_{\Omega_{s_\pm}}\left(\nabla + \nabla^t\right)(\vec{u}_{\Omega_{s_\pm}}). \end{aligned}$$

4. Inversion scheme

In this section, we describe the inversion scheme employed for imaging the interface. Additional hypotheses are made on the admissible shapes of the interface: we assume that it can be determined by its height, meaning that it can be represented by a function. More precisely, for a given set of points $\{x_i\}_{1\le i\le n_\Sigma}$ within the interval I bounded by the interface extremities (which are assumed to be known), and for some interpolation functions $\widehat{\boldsymbol{\phi}} = \{\widehat{\phi}_i\}_{1\le i\le n_\Sigma}$, we consider

$$\boldsymbol{\mathcal{U}}_{\text{admissible}} = \left\{ \Sigma = \{(x, f(x)), \quad x \in I, \quad f = \sum_{i=1}^{n_\Sigma} \xi_i \hat{\phi}_i \right\}.$$

Moreover, we only consider variations of the interface shape along the vertical component $\vec{e}_y$ of $\mathbb{R}^2$. Then, the direction $\vec{h}$ has just a vertical component, which can be interpolated using the basis $\widehat{\boldsymbol{\phi}}$:

$$\vec{h}(x) = \sum_{i=1}^{n_\Sigma} \vec{h}(x_i)\widehat{\phi}_i(x)\vec{e}_y.$$

Therefore, one can write $J(\Sigma) \equiv J(\Xi)$ with $\Xi = (\xi_1, \ldots, \xi_{n_\Sigma})$. For $\Xi^0 \in \mathbb{R}^{n_\Sigma}$, the gradient descent algorithm can be written as:

$$\Xi^{k+1} = \Xi^k - \tau\Big(\nabla_\Xi J_d(\Xi^k) + \eta \nabla_\Xi R(\Xi^k)\Big), \quad \text{where } \tau > 0 \text{ is the descent step} \tag{6}$$

and the components of the gradient of the misfit terms are $\dfrac{\partial}{\partial \xi_i} J_d(\Xi) = \displaystyle\int_\Sigma \mathrm{Re}(j(\Sigma))\, \hat{\phi}_i\, (\vec{n} \cdot \vec{e}_y)\, ds.$

5. Numerical results

To generate imaging results, we employed the Open Source finite element library FreeFEM, as introduced by Hecht (2012). This tool served for generating the mesh of the computational domain, the numerical simulation of wave propagation and for the implementation of the inversion scheme.

Figure 2 illustrates the wave propagation in both the dam and water media under two distinct source excitations, in the presence of Perfectly Matched Layer (PML) regions. This simulation highlights the proper implementation of outgoing conditions, showcasing the transition of waves to evanescent behavior upon entering PML layers, as well as the transition between elastic and acoustic waves.

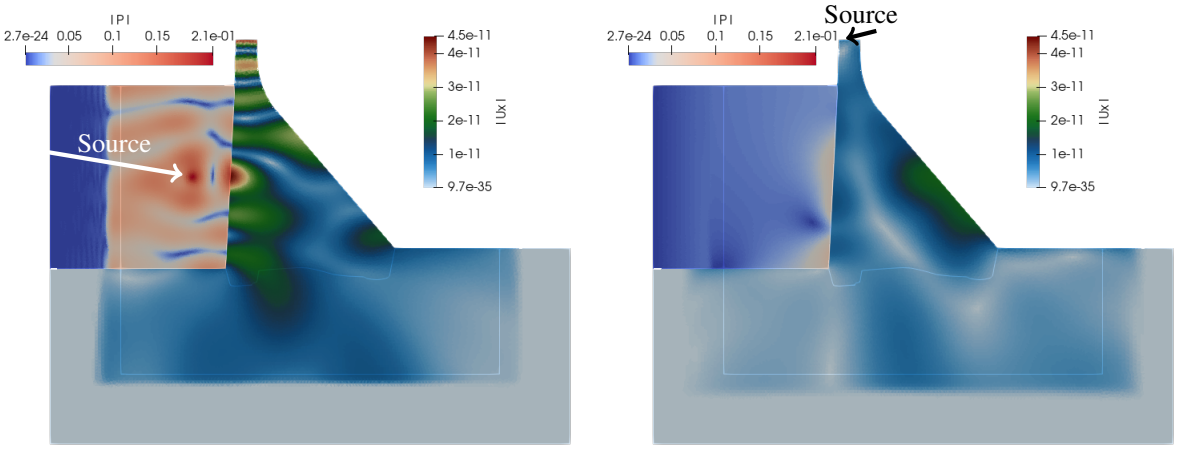

(a) Excitation of the dam structure from a source in the water.

(b) Excitation of the dam structure from a source on the dam crest.

Figure 2: Simulation of the horizontal response in the dam structure and water pressure under different excitations: (a) Excitation from the water, (b) Excitation from the dam crest, in the presence of PML layers.

In the following reconstruction results, we present a zoomed-in section of the interface area for clarity as illustrated in Fig. 3. Additionally, we initialize the algorithm with a straight line connecting the extremities of the interface, assumed to be known. The mesh is dynamically updated at each iteration, by varying the interface based on the descent direction given by equation (6). We propose two ways to evaluate the reconstruction error: first, by calculating the surface area between the reconstructed and exact interfaces (referred to as "Error," expressed in m^2), and second, by determining the maximum difference gap between the two curves (referred to as "ErrorMax," expressed in meters).

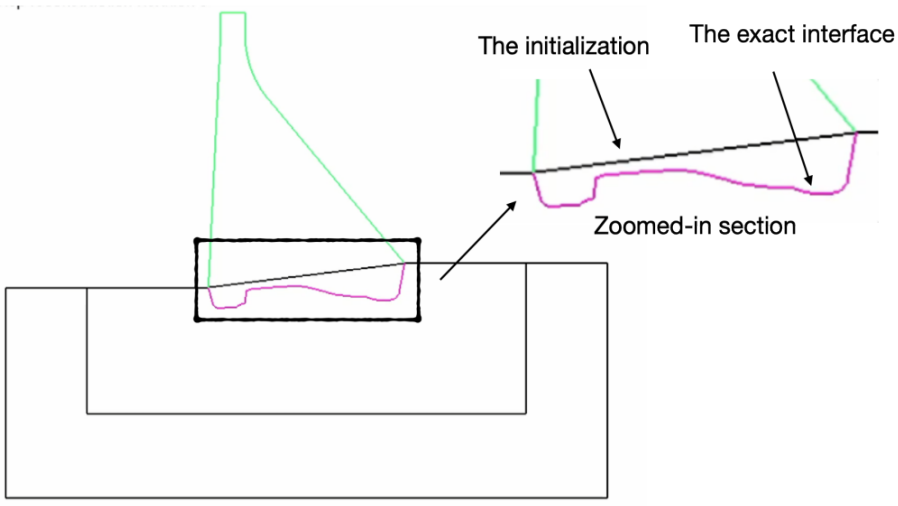

Figure 3: Illustration of the zoomed-in section of the interface area, the considered initialization and the exact interface.

Figure 4 illustrates the numerical reconstruction of the dam-rock interface using a measurement configuration closely resembling an on-site experiment. Thirteen sources were employed (5 on the upstream and downstream faces and 3 on the crest) with 90 receivers on each side. Frequencies ranged from 100Hz to 300Hz in 50Hz increments. Three different

noise levels (δ) were considered to simulate realistic on-site conditions. The evolution of the cost functional with respect to the iteration is also presented for each noise level, providing insights into the inversion process.

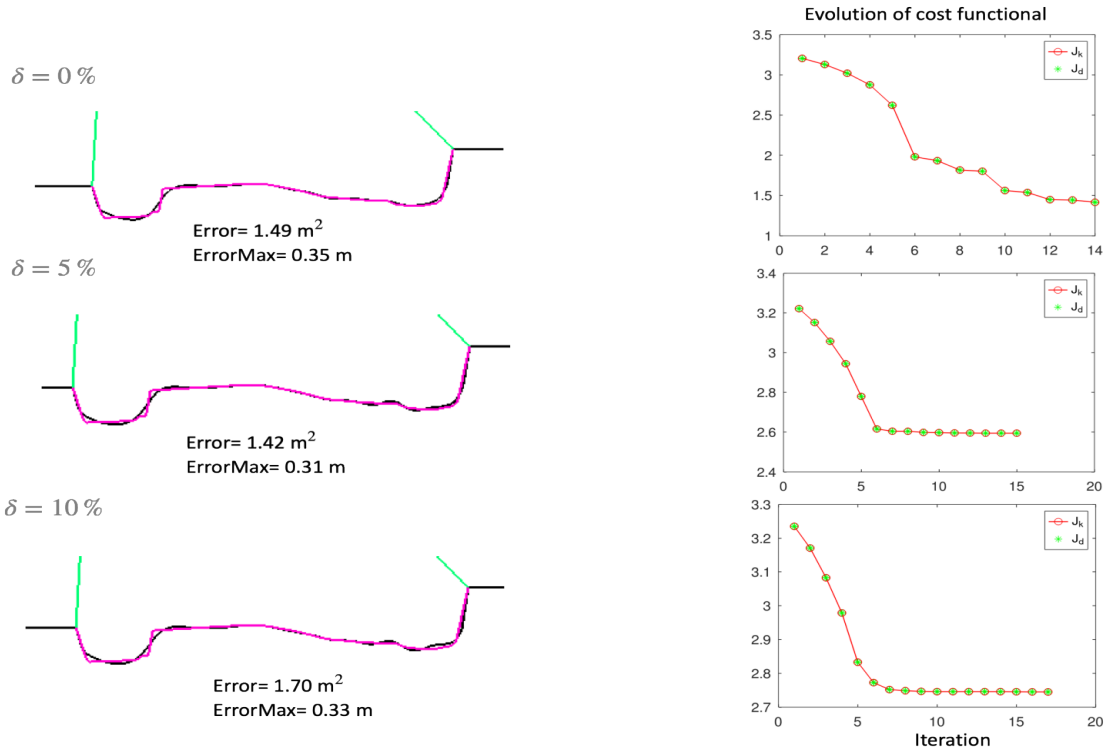

Figure 4: Reconstruction of the interface from measurements obtained by 13 sources (5 on each side and 3 on the crest) with 90 receivers on each side, using frequencies ranging from 100Hz to 300Hz in increments of 50Hz and for three levels of noise δ.

The results in Fig. 4 demonstrate the method capability to provide a high-resolution image of the dam-rock interface and its accuracy in retrieving the shape of the exact interface in the presence of noise.

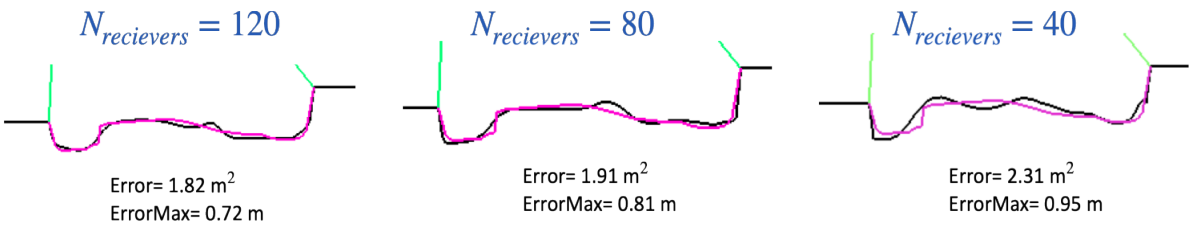

Figure 5: Reconstruction of the interface from measurements obtained by a single source positioned on the crest with different number of receivers positioned equitably at each side and using a single frequency of 150Hz, with a noise level of $\delta = 3\%$.

The use of a single source and a single frequency yielded satisfactory results, as described in Fig. 5 for a source on the crest and in Fig. 6 for a source in the water. These tests illustrate the reconstruction as the number of receivers decreases, while maintaining a noise level of $\delta = 3\%$. This testing highlights the method robustness and efficiency even with even with limited receiver configurations and a single frequency.

The positioning of receivers is tested in the experiment detailed in Fig. 7. At a constant number of receivers (5 at each side), we vary their positions at the top, middle, and bottom on each side and using frequencies 100, 150, and 200Hz. The outcomes reveal unsatisfactory reconstruction when the receivers are placed at the upper part of either side of the dam.

6. Conclusion

In this work, we have presented a method for processing geophysical measurements to construct a high-resolution image of the dam-rock interface through the inversion of a full elasto-acoustic model. In initial tests on synthetic data, we achieved satisfactory results, obtaining an interface close to the exact solution even with a limited number of measurement

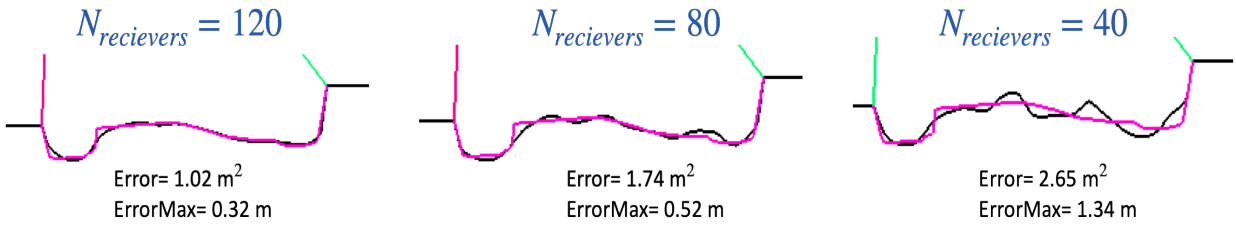

Figure 6: Reconstruction of the interface from measurements obtained by a single source positioned in the water with different number of receivers positioned equitably at each side and using a single frequency of 150Hz, with a noise level of $\delta = 3\%$.

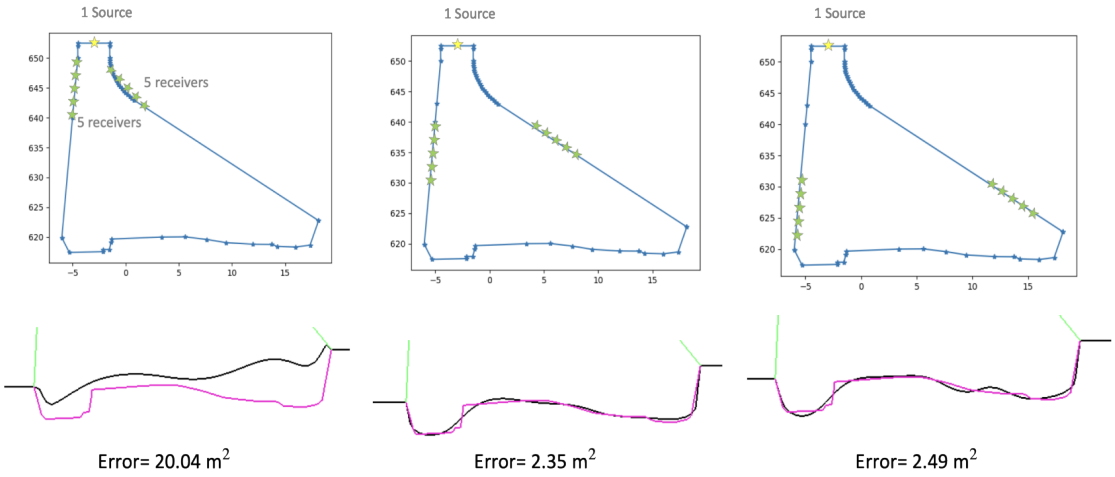

Figure 7: Reconstruction of the interface from measurements obtained by a single source positioned on the crest, with five receivers on each side, located at the top, middle, and bottom on each side, using frequencies 100, 150, and 200Hz, with a noise level of $\delta = 3\%$.

points and in the presence of noise in the measurement. It is advisable to position receivers at the bottom of the upstream and downstream faces for improved algorithm robustness. Ongoing work involves incorporating dissipation considerations into the model and conducting sensitivity tests for various acquisition parameters (receiver positions, source points, frequencies, noise levels, etc.). Future efforts will involve robustness tests for potential deviations from modeling assumptions or imprecise a priori information. Estimation of parameters, such as material characteristics, and application to real on-site measurements, will be explored.

7. REFERENCES

Allaire, G. and Schoenauer, M., 2006. *Conception optimale de structures*. Mathématiques et Applications. Springer Berlin Heidelberg.

Cea, J., 1986. "Conception optimale ou identification de formes, calcul rapide de la dérivée directionnelle de la fonction coût". *M2AN - Modélisation mathématique et analyse numérique*, Vol. 20, No. 3, pp. 371–402.

Hecht, F., 2012. "New development in freefem++". *J. Numer. Math.*, Vol. 20, No. 3-4, pp. 251–265. ISSN 1570-2820. URL `https://freefem.org/`.

Lailly, P., 1983. "The seismic inverse problem as a sequence of before stack migrations". In J.B. Bednar, E. Robinson and A. Weglein, eds., *Conference on Inverse Scattering—Theory and Application*. SIAM, Philadelphia, pp. 206–220.

Michler, C., Demkowicz, L., Kurtz, J. and Pardo, D., 2007. "Improving the performance of perfectly matched layers by means of hp-adaptivity". *Numerical Methods for Partial Differential Equations*, Vol. 23, No. 4, pp. 832–858.

Tarantola, A., 1984. "Inversion of seismic reflection data in the acoustic approximation". *Geophysics*, Vol. 49, No. 8, pp. 1259–1266.

8. RESPONSIBILITY NOTICE

The authors are solely responsible for the printed material included in this paper.